CCCARD2014-051

PRELIMINARY COMPARISON OF TRANSPORT CODES APPLIED TO A SECOND-GENERATION PT-SCWR LATTICE

R. Farkas¹ and E. Nichita¹University of Ontario Institute of Technology, Ontario, Canada

Abstract

The Pressure-Tube Supercritical Water Cooled Reactor (PT-SCWR) is being developed in Canada as Canada's contribution to the Generation IV International Forum (GIF). A two-dimensional lattice benchmark has been previously developed to assess the applicability of various lattice physics codes to the PT-SCWR design. This work summarizes the benchmark results for two lattice codes: Serpent, a stochastic transport code, and DRAGON, a deterministic transport code. Specifically, k-effective, spectrum and multi-group macroscopic cross-sections as a function of burnup are compared. Preliminary results show a 4 mk difference in the reactivity values and a maximum 6% difference in two-group macroscopic cross sections.

1. Introduction

The Pressure-Tube Supercritical Water Cooled Reactor (PT-SCWR) currently being developed in Canada is part of the Generation IV International Forum (GIF) efforts to develop future nuclear-power systems. The PT-SCWR consists of a square vertical array of fuel channels composed of a pressure tube and an inner ceramic thermal insulator each containing 78-element Th-Pu fuel bundles cooled by light water. The array of channels is immersed in a heavy water moderator within a non-pressurized cylindrical vessel. A two-dimensional lattice benchmark has been previously developed to assess the applicability of various lattice physics codes to the PT-SCWR design; the benchmark is in part based on the specifications outlined in reference [1].

This work summarizes the application of two lattice codes to the established PT-SCWR lattice benchmark. Specifically, the results produced by Serpent [2] a stochastic (Monte Carlo) transport code are compared to those produced by DRAGON [3] a deterministic lattice code. The two codes are compared on the basis of the two-group macroscopic cross-sections they produce, the predicted reactivity as a function of burnup and the flux as a function of energy (i.e. spectrum). Additionally, comparisons to the typical, natural-uranium-fuelled, CANDU lattice are made throughout the paper.

2. The PT-SCWR lattice benchmark

The PT-SCWR lattice has been updated periodically as the design has been refined [4]. The lattice geometry analyzed in this work corresponds to an intermediate-generation of the lattice design. Similar benchmarking studies have been performed for the equivalent design [5] as well as for previous versions of the lattice [6].

2.1 Benchmark geometry

Figure 1 provides a scale comparison between the typical CANDU, Figure 1a, lattice and the PT-SCWR lattice geometry specified by the benchmark, Figure 1b. Many of the differences between the traditional CANDU lattice and the PT-SCWR lattice are immediately apparent. For instance, where the CANDU has the concentric pressure and calandria tubes separated by an annulus gap to reduce the heat lost from the fuel channel to the moderator, the PT-SCWR has only a pressure tube in direct contact with the moderator. Within the pressure tube the PT-SCWR uses a thermal insulator (light coloured region within the pressure tube in Figure 1b) the purpose of which is to reduce heat loss to the moderator. A thin liner tube, located between the insulator and the fuel assembly, serves to protect the insulating layer from mechanical wear. Another distinguishing feature of the PT-SCWR lattice is the use of three distinct pin radii including a large-radius non-fuel centre pin. The non-fuel centre pin has been included with the intention of reducing the coolant void reactivity (CVR).

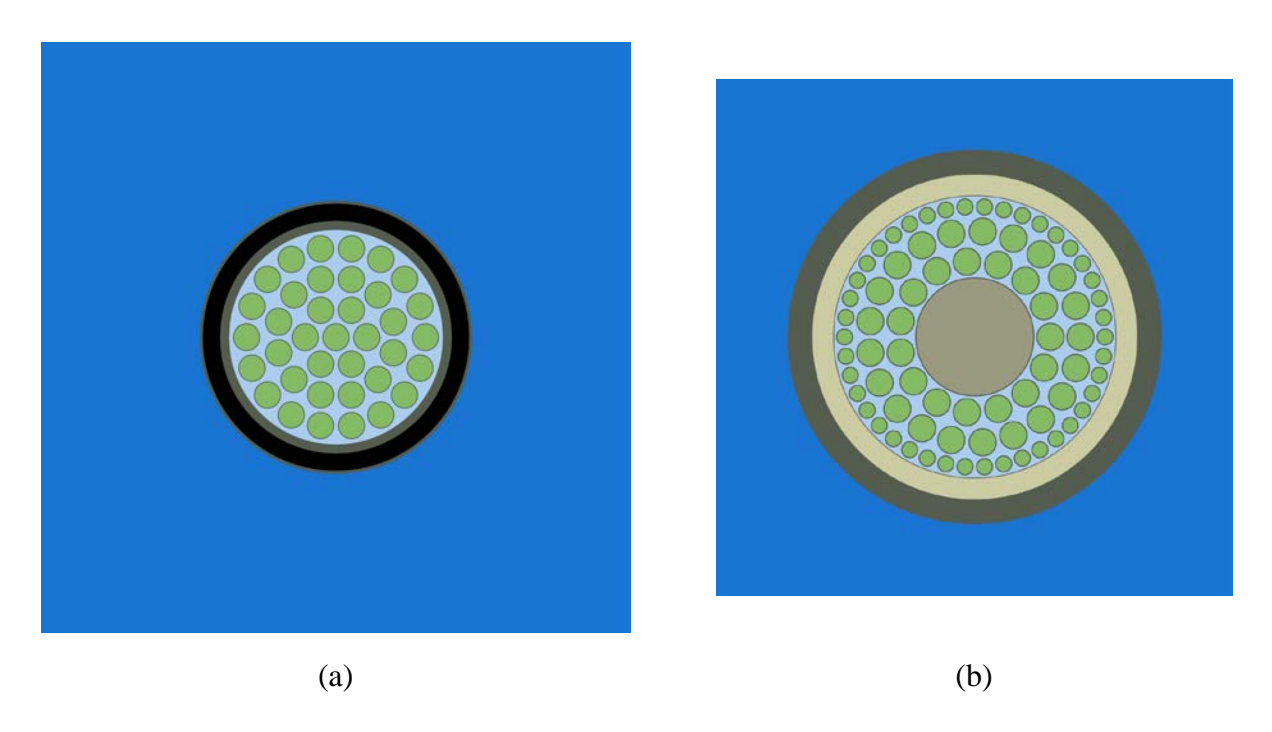


Figure 1 Comparison of typical CANDU lattice with a 37-element bundle (a) to the 78-element PT-SCWR benchmark – to scale.

The specific dimensions of the components that constitute the 78-fuel-element lattice cell in Figure 1b are summarized in Table 1.

Table 1 The geometry of the PT-SCWR lattice cell – dimensions of the components [1].

Centre pin					
Number	1				
Pin radius	2.82 cm				
Pitch circle radius	0.00 cm				
Cladding thickness	0.06cm				
Inner pins					
Number	15				
Pin radius	0.62 cm				
Pitch circle radius	3.66 cm				
Cladding thickness	0.06 cm				
Intermediate pins					
Number	21				
Pin radius	0.62 cm				
Pitch circle radius	5.11 cm				
Cladding thickness	0.06 cm				
Outer pins					
Number	42				
Pin radius	0.35 cm				
Pitch circle radius	6.30 cm				
Cladding thickness	0.06 cm				
Liner tube					
Inner radius	6.80 cm				
Outer radius	6.85 cm				
Insulator					
Inner radius	6.85 cm				
Outer radius	7.85 cm				
Pressure tube					
Inner radius	7.85 cm				
Outer radius	9.05 cm				
Lattice					
Lattice pitch	25.00 cm				

2.2 Benchmark material composition

The composition and temperature of each component are presented in Table 2. According to the benchmark specifications, the coolant properties change as a function of the position along the channel. The values presented in Table 2 correspond to values 0.5 m from the channel inlet.

Table 2 Composition of benchmark materials

Component	Material	Composition [wt%]	Density [g/cm ³]	Temperature [K]
Centre pin	Zirconia	Zr: 72.3; O: 27.7;	5.37	Same as coolant
Insulator			1.29	600
Fuel*	PuO ₂ /ThO ₂	O-16: 12.042; O-17: 0.005; Pu-238: 0.315; Pu-239: 5.959; Pu-240: 2.633; Pu-241: 1.747; Pu-242: 0.814; Th-232: 76.456;	9.88	900
Pin cladding	Zr-modified 310 stainless steel (H2) C: 0.034; Si: 0.51; Mn: 0.74; P: 0.016; S: 0.002; Ni: 20.82; Cr: 25.04; Fe: 51.738; Mo: 0.51; Zr: 0.59;	7.00	900	
Liner tube		Cr: 25.04; Fe: 51.738; Mo: 0.51;	7.90	Same as coolant
Coolant [†]	Light water	H ₂ 0(%):100.0;	Variable 0.59254	Variable 600
Pressure tube	Excel (zirconium alloy)	Sn: 3.5; Mo: 0.8; Nb: 0.8; Zr: 94.9;	6.52	600
Moderator	Heavy water	D ₂ O(%): 99.833; H ₂ O(%): 0.167;	1.8051	300

^{*} Fuel composition specified is for fresh fuel.

[†] The coolant properties vary as a function of the distance along the fuel channel (height) the values given correspond to the values simulated in this analysis.

3. Lattice models

The geometry and compositions as specified above are represented as two-dimensional models in DRAGON and Serpent. The models as simulated appear in Figure 3. Both models:

- Use nuclear data from JEFF3.1.
- Simulate an infinite lattice (no leakage), and
- Burn the lattice to 25 MWd/kg at a power density of 29.2 W/g.

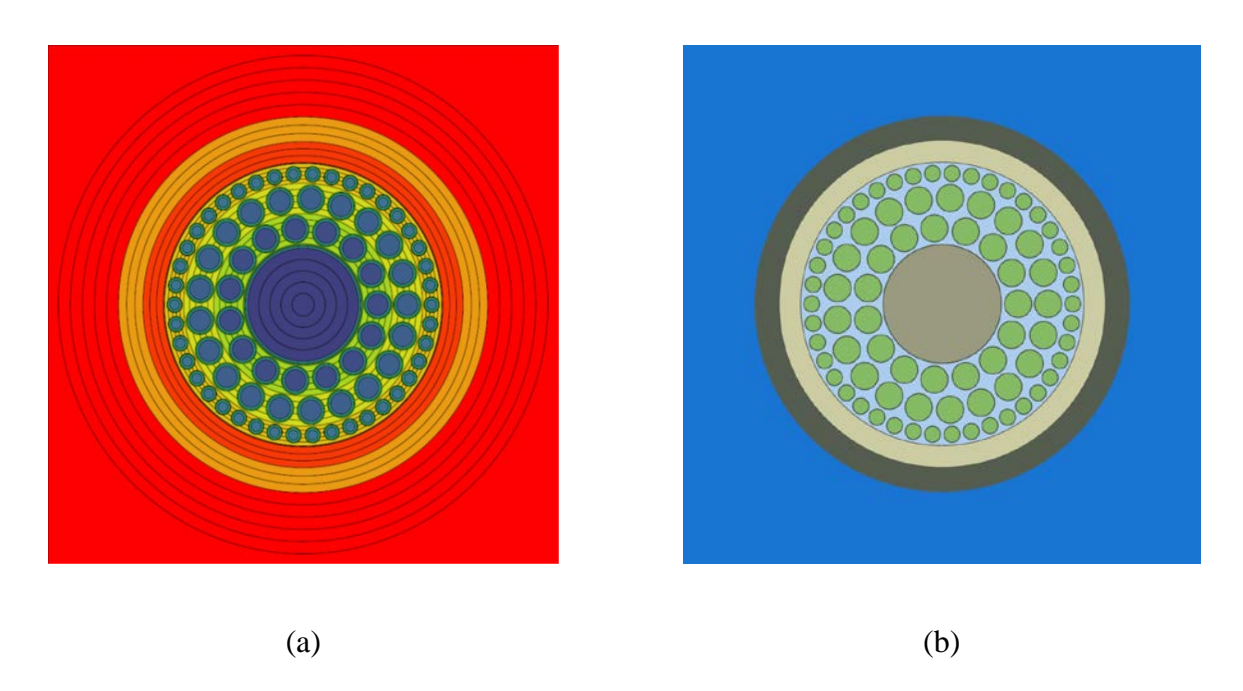


Figure 3 Comparison of lattice models for DRAGON (left) and Serpent (Right).

3.1 DRAGON model

The deterministic solution to the neutron transport equation is obtained by the collision probability method as implemented in the lattice code DRAGON, version 3.05. The transport equation is solved in 69 energy groups using the WIMSD-formatted WLUP multi-group library based on JEFF3.1 [7] Figure 3a gives an indication of the spatial discretization used in the transport calculation. The model assumes an infinite lattice using 'white' boundary conditions. Previous work has identified the self-shielding option used to be of importance [6]. As such, it is worth noting that the 'No Livolant-Jeanpiere' (NOLJ) self-shielding option was used.

3.2 Serpent model

The stochastic solution to the neutron transport equation is solved using the code Serpent, version 1.1.14. The nuclear data used corresponds to JEFF3.1 library [2] packaged with the Serpent distribution. The model used reflective boundary conditions. The Serpent simulation used 2500 active cycles with 2000 neutrons every cycle for a total of 5×10^6 active histories each burnup step. To accommodate the model within the available memory it was necessary to relax the energy grid reconstruction tolerance to 4×10^{-4} . The manual indicates that for most problems that a tolerance less

than 10^{-3} will not significantly impact results [2]; the relaxation is mentioned here only for completeness.

4. Results

4.1 Infinite multiplication factor

The reactivity curve, k-infinity as a function of burnup, for both DRAGON and Serpent are plotted in Figure 4. Serpent is a stochastic code, and hence its prediction of k-infinity is associated with some degree of statistical error. Because the statistical error is small relative to the size of the data points in Figure 4 indication of the uncertainty is omitted from the curve. However, for completeness, the Serpent-reported statistical uncertainty in k-infinity varied slightly around 2×10^{-4} for each burnup step. The variation in the reactivity difference at the top of Figure 4 gives an indication of the magnitude of the error.

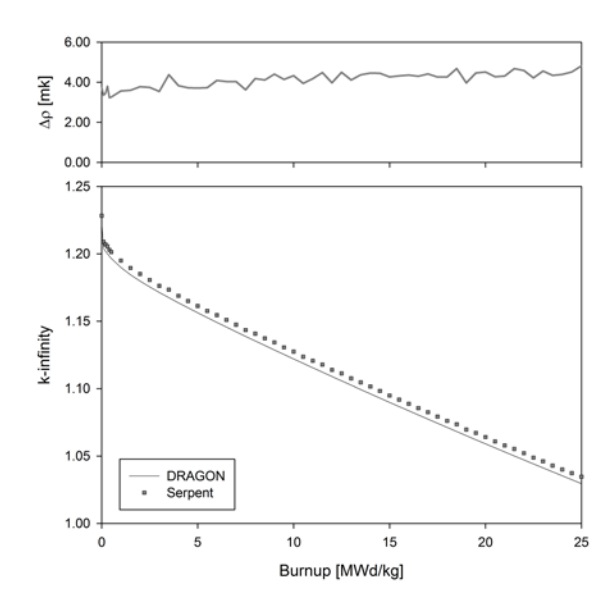


Figure 4 The PT-SCWR infinite lattice reactivity curve, k-infinity as a function of burnup as predicted by DRAGON and Serpent.

Serpent predicts a more reactive lattice when compared to Serpent. The difference is largely constant at ~4mk over the 25 MWd/kg the lattice was burned with the difference increasing slightly as the lattice burns.

4.2 Spectrum

The fresh lattice spectrum comparison between DRAGON and Serpent is presented in Figure 5. The energy per unit lethargy is presented in 69 bins. It is important to note that while DRAGON solves the transport equation in 69 energy groups Serpent is a continuous energy Monte Carlo code. The results from the Serpent calculation are simply output in the 69 energy group structure used by WLUP [8] for the purposes of comparison. To further facilitate comparison the Serpent cell fluxes have been normalized to the total DRAGON integrated flux. Again, the statistical uncertainty in the energy

dependent flux is small compared to the difference between DRAGON and Serpent and therefore omitted from the plot.

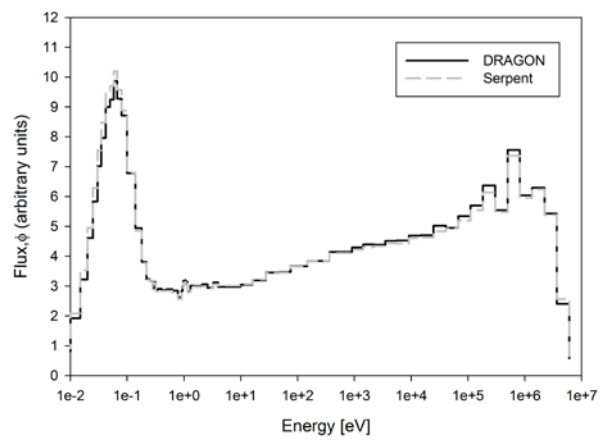


Figure 5 Comparison of cell flux in each of the of energy groups corresponding to those used for the DRAGON deterministic calculation.

Overall, DRAGON and Serpent agree in terms of spectrum with DRAGON predicting a slightly harder spectrum than Serpent.

4.3 Two-group cross-sections

Typical CANDU analysis calls for homogenized two-group macroscopic cross-sections to be generated for use in full-core diffusion calculations. The fast and thermal groups are usually delineated at 0.625 eV. While it is beyond the scope of this work to comment on whether or not only two energy groups are sufficient to capture the salient full-core physics phenomena in a PT-SCWR diffusion calculation it is nevertheless illustrative to compare some of the important two-group macroscopic cross-sections. Specifically, the two-group absorption, production and scattering cross-sections calculated by DRAGON and Serpent are compared in the following sections.

4.3.1 Two-group absorption cross-section

The two-group macroscopic absorption cross-sections are presented with the attendant statistical uncertainty in Figure 6; the fast group is on the left and the thermal group is on the right. In both cases, fast and thermal, DRAGON predicts a greater likelihood of absorption within the cell by approximately 2% for the fast group and approximately 4% for the thermal group. Again, the results are largely insensitive to burnup showing a consistent difference throughout the 25 MWd/kg burnup range.

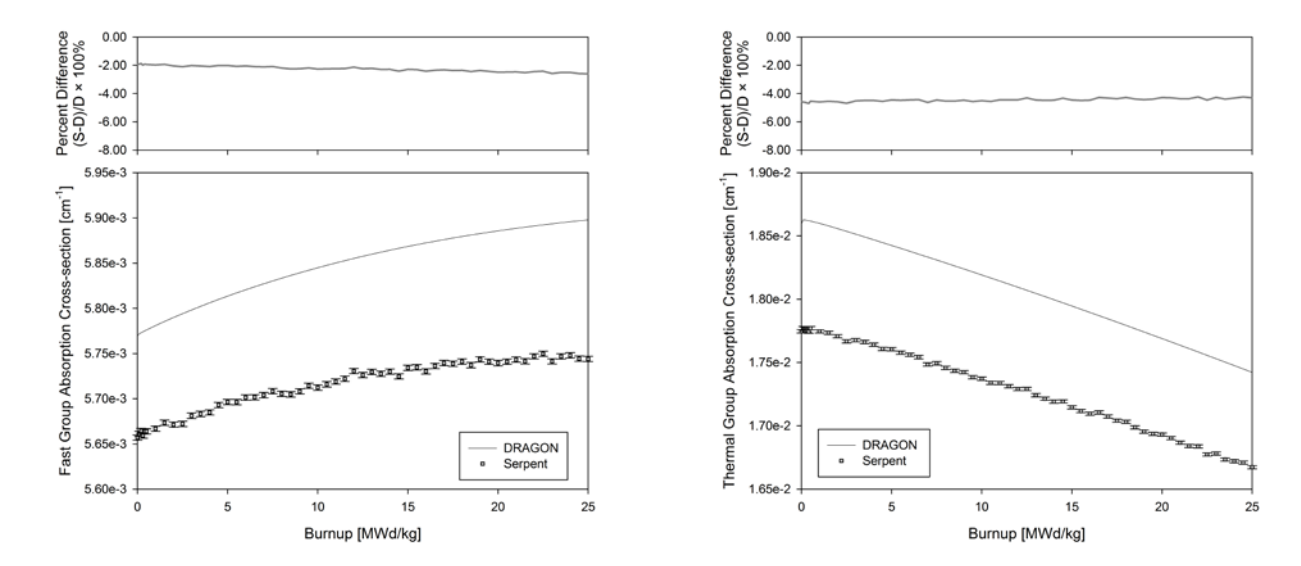


Figure 6 Comparison of the homogenized two-group macroscopic absorption cross-section for the fast group (left) and the thermal group (right).

4.3.2 <u>Two-group production cross-section</u>

The two-group macroscopic production cross-sections are presented in Figure 7. In the case of the production cross-section DRAGON and Serpent agree well for the fast group but by comparison disagree markedly, by approximately 6%, in the thermal case where DRAGON predicts a higher production cross-section.

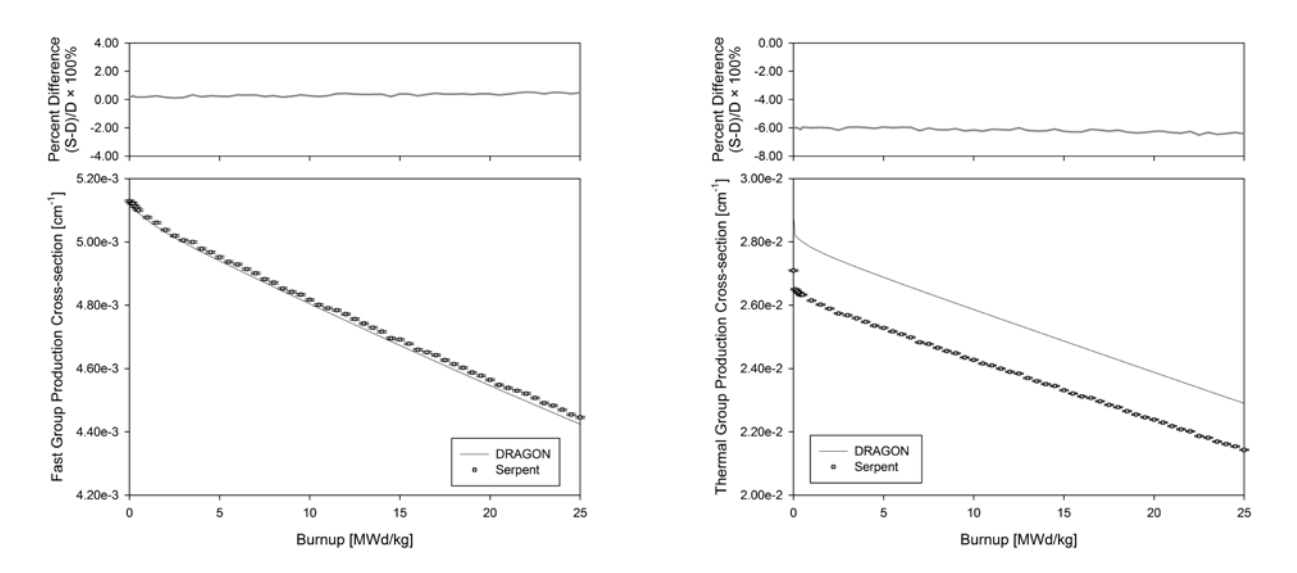


Figure 7 Comparison of the homogenized two-group macroscopic production cross-section for the fast group (left) and the thermal group (right).

4.3.3 Group transfer cross-section

The group transfer cross-sections, up-scatter and down-scatter, are presented in Figure 8. Generally, there is agreement on the order of the statistical uncertainty in the case of down-scattering with little difference between DRAGON and Serpent. The agreement however does not extend to the case of up-scattering where the difference between DRAGON and Serpent ranges between 6% and 8% with DRAGON predicting scattering into the fast group from the thermal group as more likely. Because the up-scatter cross-section represents the likelihood of a rare event there is noticeable statistical uncertainty in the Serpent predicted cross-section.

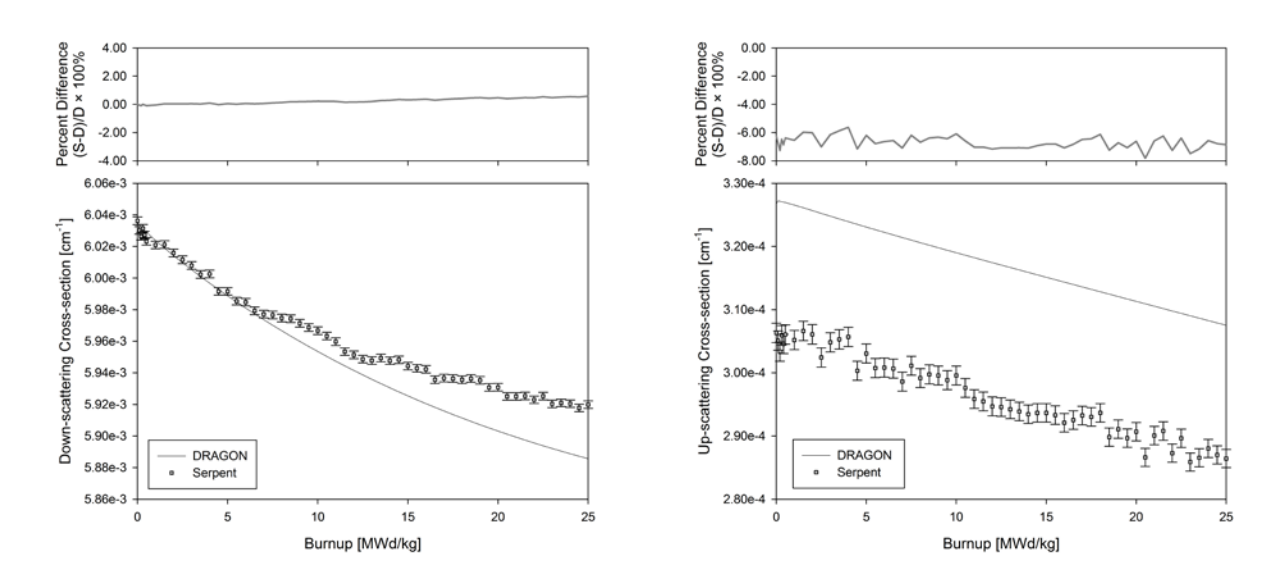


Figure 8 Comparison of the homogenized two-group macroscopic group transfer cross-sections for down-scattering (left) and up-scattering (right).

4.4 Summary of results

The previous sections outline results of a preliminary comparison of the lattice codes DRAGON and Serpent as applied to a PT-SCWR lattice. In general there is agreement particularly in the reactivity and spectrum with the reactivity agreeing to within ~4 mk. Furthermore, any differences seem to be largely insensitive to burnup over the 25 MWd/kg range considered implying a similarity between DRAGON and Serpent results in the solution of the Bateman equations. With respect to the two-group homogenized cross-sections DRAGON predictions are higher for both absorption and production which perhaps implies some cancellation of errors leading to the close agreement in k-infinity as a function of burnup.

5. Conclusion

A comparison of the lattice codes DRAGON and Serpent has been performed by applying both to a two-dimensional lattice benchmark of the PT-SCWR. The comparison primarily focused on the application of the codes to reactivity, spectrum and the production of select two-group homogenized cross-sections. The codes compare favourably in terms of the infinite lattice reactivity as a function of burnup and spectrum. In terms of the two-group cross-sections examined the codes demonstrated

differences to a maximum of around 6%. The differences in cross-sections could be reconciled with close agreement in infinite lattice reactivity if some cancellation of errors were considered.

6. Acknowledgement

Funding to the Canada Gen-IV National Program was provided by Natural Resources Canada through the Office of Energy Research and Development, Atomic Energy of Canada Limited, and Natural Sciences and Engineering Research Council of Canada.

7. References

- [1] J. Pencer, M. Edwards and N. Onder, "Axial and radial graded enrichment options for the Canadian SCWR", <u>The 3rd China-Canada Joint Workshop on Supercritical-Water-Cooled Reactors</u>, Xi'an, China, 2012 April 18-20.
- [2] J. Lappanen, "Serpent a continuous-energy Monte Carlo reactor physics burnup calculation code", User's Manual, 2013.
- [3] G. Marleau, A. Herbert and R. Roy, "A user guide for DRAGON release 3.06L", IGE-174 Rev. 12, 2013.
- [4] J. Pencer and A. Colton, "Progression of the Lattice Physics Concept for the Canadian Supercritical Water Reactor", <u>Proceedings of the 34th Annual Conference of the Canadian Nuclear Society</u>, Toronto, Ontario, 2013 June 9-12.
- [5] D. Hummel, S. Langton, M. Ball, D. Novog and A. Buijs, "Description and Results of a Two-Dimensional Lattice Physics Code Benchmark for the Canadian Pressure Tube Supercritical Water-cooled Reactor (PT-SCWR)", <u>Proceedings of the 34th Annual Conference of the Canadian Nuclear Society</u>, Toronto, Ontario, 2013 June 9-12.
- [6] G. Harrisson and G. Marleau, "Computation of a Canadian SCWR unit cell with deterministic and Monte Carlo codes", <u>PHYSOR 2012</u>, Knoxville, Tennessee, 2012.
- [7] <u>https://www-nds.iaea.org/wimsd/downloads2.htm</u>, retrieved January 29, 2014.
- [8] Leszczynski, F., López Aldama, D., Trkov, A., "WIMS-D library update: final report of a coordinated research project", Vienna, International Atomic Energy Agency, 2007.